

## HUMAN-BODY MODELING AND POSITION SPECIFICATION FOR FORENSIC AUTOPSY DATA VISUALIZATION

Junki Mano<sup>†</sup>      Masahiro Toyoura<sup>†</sup>      Xiaoyang Mao<sup>†</sup>  
Hideki Shojo<sup>†</sup>      Noboru Adachi<sup>†</sup>      Issei Fujishiro<sup>††</sup>

<sup>†</sup>University of Yamanashi      <sup>††</sup>Keio University

### ABSTRACT

This paper proposes the methods for creating a human-body model that reflects individual victim characteristics and obtaining position information on the human-body model for the purpose of forensic autopsy data visualization. Although modern imaging technologies, such as CT and MRI, make it possible to obtain fine volumetric human-body model, these technologies are still not widely used in the real forensic autopsy sites due to the cost. To enable a forensic specialist to easily create 3D models of victims, we propose a new method which uses an affordable depth-sensing camera and requires few user interactions. To visualize the autopsy data directly on a 3D model, we also propose a method for specifying a position on the 3D model without impeding the progress of the autopsy procedure.

### 1. INTRODUCTION

Forensic autopsy reports play significant roles in court decisions. It includes data on any injuries apparent on the body subject to the autopsy, photographs of the corresponding injury locations, and the findings of the medical examiner who performed the autopsy. Forensic autopsy reports contain substantial amounts of technical terminology and unfamiliar statements. For jurors without any background in legal constructs or autopsy procedures, then, it can be difficult to understand the nature of the injuries. Computer graphics (CG) technology can be useful in making autopsy results more intuitive, as they provide direct visual renderings of injuries and other conditions on a 3D CG model of the victim.

Figure 1 shows an example of the type of forensic autopsy data visualization that this study addresses. The visualization method involves associating injury data and photographs from an actual forensic autopsy to injury locations on a human-body model that reflects the unique individual characteristics of the body subject to the autopsy. Selecting a site on the human-body model brings up the associated forensic autopsy data in a new window and renders a direct visualization on the human-body model via texture mapping.

This visualization approach requires two primary steps: building a human-body model that reflects the individual characteristics of the body subject to the autopsy and obtaining position information on the human-body model, thus enabling the mapping of

forensic autopsy data. Researchers have attempted to create human-body models using the “virtual autopsy” [1] approach, which involves performing a CT scan on the body and analyzing the results on a computer. But these technologies are still not widely used in the real forensic autopsy sites due to the cost for purchasing and maintaining 3D imaging instruments. To obtain forensic autopsy data from the source in real time and associate the data with a corresponding human-body model, one would also need to be able to gather position information during the autopsy without impeding the progress of the autopsy procedure.

To address these needs, this study aims to propose a method for using a depth-sensing camera and a pointing device to create a human-body model that reflects individual characteristics and allow users to obtain position information on the human-body model during the course of an autopsy.

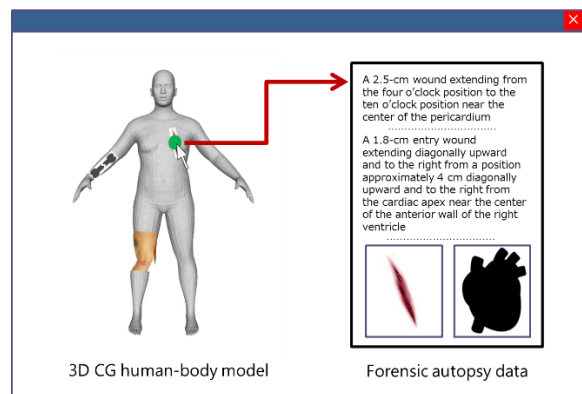


Figure 1: An example of forensic autopsy data visualization

### 2. RELATED RESEARCH

#### Input system for forensic autopsy data

Boussejra et al. [2] proposed an input system for forensic autopsy data. The system was built with a mark-up language LMML (legal medicine mark-up language) which is designed for describing forensic autopsy data. A medical examiner can quicker and smoother input the data than the conventional manual description. The modeling and position specification technologies proposed in this paper provides the key technology for implementing the browser for viewing LMML data in 3D.

### Human-body modeling

Xi et al. [3] used non-numerical attributes like gender, age, race, marital status, and occupation to predict body shapes and build human-body models accordingly. Although the research makes it possible for scientific criminal investigators without any photographs of a given suspect to get an estimation of the individual's face and body shape based solely on age, occupation, and other characteristics, the approach is not an effective means of creating human-body models that reflect specific individual characteristics. Anguelov et al. [4], meanwhile, proposed a method for creating human-body models by using a training database of learned posture models. These approaches, however, are not effective means of creating human-body models that reflect specific individual geometric characteristics.

Allen et al. [5] used a standard model with an average body shape and body scan data to create a human-body model. As scan data is susceptible to the effects of noise and data damage, Allen et al. began by preparing a standard model free of noise and incomplete surfaces and then deformed the model in accordance with the scan data. This made it possible to create a human-body model that not only conformed to the shape of the scan data but also eliminated the chances of any noise or incomplete surfaces undermining the results. The Allen et al. [5] method, which enables the creation of human-body models that feature individual characteristics and a full-body mesh, thus provided a useful basis for our study. Drawing on the Allen et al. [5] approach, we prepared a standard model and deformed it based on data readings from a depth-sensing camera to create a human-body model that reflects individual characteristics.

### 3D position specification

To obtain position information on the 3D human-body model, thereby enable the mapping of autopsy data onto the 3D model, we need a method allowing the user to easily specify a position on the 3D model during the process of autopsy. As means for allowing interaction between the real space and the three-dimensional space, there are methods to use gestures and mobile devices [6] [7]. These researches, as the means of interaction are effective, but are not tailored for acquiring position information on any 3D space.

## 3. PROPOSED METHOD

### 3.1. Overview

Figure 2 depicts the overview of the proposed method. Before the forensic autopsy begins, we use Kinect RGB-D sensor mounted on the ceiling of the autopsy room to obtain a scan of the body subject to the autopsy and then use the scan data to create a human-body model that reflects the individual characteristics of the body. Next, the medical examiner proceeds with the forensic autopsy and notes findings. When recording data or findings on a given injury, the medical examiner specifies the position of the injury by illuminating the site with a laser pointer. The RGB-D sensor captures images of sites that the

examiner has specified, and our system then automatically converts that input into position information on the human-body model.

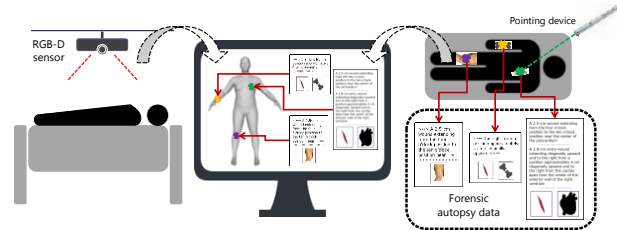


Figure 2: Overview of the proposed method

### 3.2. Human-body modeling

The proposed method generates a human-body model in the following 2 steps:

1. Obtain scan data via an RGB-D sensor
2. Deform the standard model based on the scan data obtained in step 1

Scan data from RGB-D sensors is susceptible to several problems, including noise that can occur during the body scan, mesh collapse in areas that the scan fails to measure correctly. Human-body models used in the visualization of forensic autopsy data also need to retain anatomic reference, which aid in the acquisition of position information from the autopsy findings. Figure 3 shows the anatomic reference points.

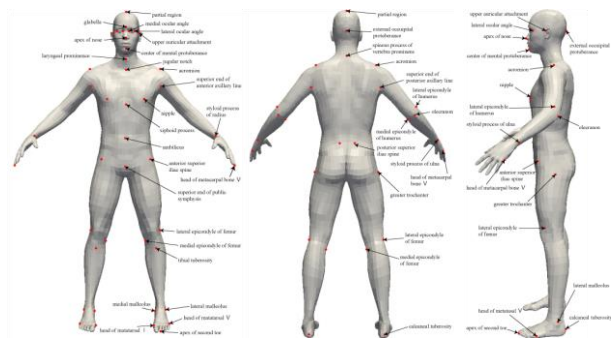


Figure 3: Anatomic reference points

When recording position information for an injury in his or her findings, the medical examiner uses the anatomic reference point(s) nearest the injury site to denote the location. Reproducing these recorded findings in a visualization would require a human-body model with the same anatomic feature points.

For these reasons, visualization cannot be generated using the scan data alone. Drawing on the Allen et al. method [5], we thus deform a standard, predefined full-body mesh model to fit the scan data. This makes it possible to generate a noise-free, incomplete surface-free human-body model that reflects individual characteristics. By predefining anatomic reference points on the standard model, our method also ensures that the resulting human-body models include anatomic reference point information. As will be described later in this section, we also predefine a skeleton on the standard model for the purpose of posture registration

The Allen et al. method [5] uses 3 error items, data error, smoothness error, and marker error of Formula 1~3, respectively, to evaluate the degree of similarity between the standard model and scan data.

$$E_d = \sum_{i=1}^n w_i \text{dist}^2(T_i v_i, D) \quad (1)$$

$$E_s = \sum_{\{i, j\} \in \text{edge}(\text{mathcal{T}})} \|T_i - T_j\|_F^2 \quad (2)$$

$$E_m = \sum_{i=1}^m \|T_{k_i} v_{k_i} - m_i\|^2 \quad (3)$$

In Formula 1, each vertex  $v_i$  in the standard model is influenced by a  $4 \times 4$  affine transformation matrix  $T_i$ .  $\text{dist}^2()$  is the minimum distances between  $n$  vertices  $v_i$  on the standard model and the vertices on scan data  $D$ . We then match the standard model with the scan data so that the total of the minimum distances is as small as possible.  $w_i$  is a weight for ensuring that the process does not link non-matching vertices. If the minimum distances is large, we decide that the correspondence between the points is not reliable (for example there is missing data on scan data  $D$ ) and we set the weight  $w_i$  to zero.

For the smoothness error of Formula 2, we determine the Frobenius norms of transformation matrices  $T_i$  and  $T_j$  with vertices  $v_i$  and  $v_j$ , which are adjacent to each other on the standard model, to calculate the amount of change. We then implement controls to produce the deformation with the minimum amount of change and thereby maintain the mesh configuration of the standard model.

For the marker error function of Formula 3, the L2 norm for  $m$  marker points  $v_{k_i}$  on the standard model and marker point  $m_i$  on the scan data are computed. We perform matching to minimize the total of the distances. The marker points in our study are the anatomic reference points from Figure 3. The final error function  $E$  is the linear combination of the three error items given above:

$$E = \alpha E_d + \beta E_s + \gamma E_m \quad (4)$$

By performing optimization processing to minimize the result of Formula (4), we obtain transformation matrix  $T$  for transforming the standard model. In Formula (4),  $\alpha$ ,  $\beta$ , and  $\gamma$  are weights for controlling the ratios of the three error functions. We deform the standard model by applying calculated transformation matrix  $T$  to the vertices of the standard model.

According to our experiments, using Allen's method [5] with a low-resolution standard model can successfully create a human-body model that closely resembled the shape of the scan data but it may fail in case of a high-resolution standard model. We observed that the reason for this problem is caused by the difference of postures. When the standard model and the scan data have very different postures, the smoothness error function  $E_s$  falls into a local solution, thus

interfering with the initial deformation procedure. We solve the problem by using the skeleton defined on the standard model to align the postures between the standard model and scan data first before starting the deformation.

Figure 4 illustrates the steps of the skeleton-based initial deformation process.

1. Transform the control points of skeleton to the corresponding positions in the scan data
2. Calculate the transformation matrix for converting the bones of the skeleton on standard model to the bones of the skeleton obtained in step 1
3. Establish a transformation matrix applicable to the vertices of the standard model and then perform the initial deformation

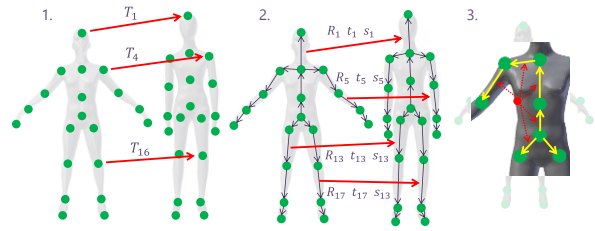


Figure 4: Overview of the skeleton-based initial deformation process

To transform the control points of the skeleton on the standard model to the corresponding points of the scan data, we use the transformation matrix obtained by optimizing the marker error function  $E_m$ . This is reasonable because the positions of markers (the anatomic reference points) are close to that of the control points. Denoting a bone of standard model and its correspondence in scan model as  $v_i$  and  $v_i'$ , respectively, the translation matrix  $t$ , scaling value  $s$ , and rotation matrix  $r$  for each bone can be computed via the following formulas:

$$t_i = v_i' - v_i \quad (5)$$

$$s_i = \frac{\|v_i' - v_j'\|}{\|v_i - v_j\|} \quad (6)$$

$$r_i = \begin{pmatrix} r_x^2(1 - \cos\theta) + \cos\theta & r_x r_y(1 - \cos\theta) + r_z \sin\theta & r_x r_z(1 - \cos\theta) + r_y \sin\theta \\ r_x r_y(1 - \cos\theta) + r_z \sin\theta & r_y^2(1 - \cos\theta) + \cos\theta & r_y r_z(1 - \cos\theta) + r_x \sin\theta \\ r_x r_z(1 - \cos\theta) + r_y \sin\theta & r_y r_z(1 - \cos\theta) + r_x \sin\theta & r_z^2(1 - \cos\theta) + \cos\theta \end{pmatrix} \quad (7)$$

$$\cos\theta = \frac{(v_i - v_j) \cdot (v_i' - v_j')}{\|v_i - v_j\| \|v_i' - v_j'\|} \quad (8)$$

$$\sin\theta = \sqrt{1 - \cos^2\theta} \quad (9)$$

$$\begin{pmatrix} r_x \\ r_y \\ r_z \end{pmatrix} = \frac{(v_i - v_j) \times (v_i' - v_j')}{\|(v_i - v_j) \times (v_i' - v_j')\|} \quad (10)$$

To deform the whole model at 3<sup>rd</sup> step, we need to determine the transformation matrix to apply to each vertex of the standard model. The transformation matrix applied to each vertex should be computed based on the most relevant bone, for example based on the transformation matrix of the closest bone.

The geodesic distance is useful if want to find the distance between two vertices on the mesh, but generally bones are defined in space rather than on mesh, so we can't use geodesic distance. Also, Euclidean distance can associate a bone to a vertex on a different part of the body, such as associating an arm to the closest side of upper body, so it is not possible to determine an appropriate transformation matrix. Therefore, we first segment the standard model using Huang et al. method [8] before using Euclidean distances to ensure the correct correspondence. Figure 5 shows the segmentation of the standard model.

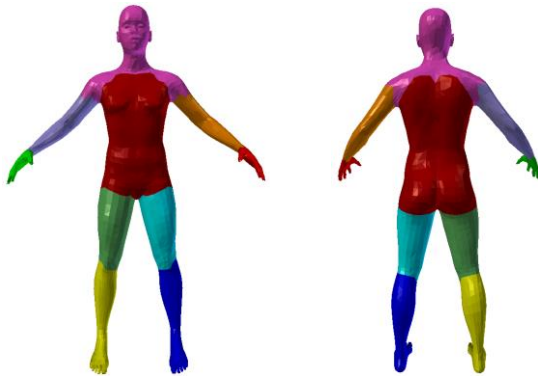


Figure 5: Segmentation of standard model

We compute the Euclidean distances between the vertex and bone according to segmentation result, and associate vertices with bones that are closest in distance and determine the transformation matrix to apply to each vertex. After that, we perform initial deformation using skeletal subspace deformation to obtain a smooth result.

With the initial model available, it is further refined by iterating the optimization process that minimize the error function given in Formula (4). Since the resolution of the standard model used is low, a low resolution model will be constructed as the result. Finally, we increase the resolution of the resulting model by using Catmull and Clark's method [9]. This method for recursively generating surfaces that approximate points lying-on mesh of arbitrary topology, so it is possible to maintain the topology of result model and increase the resolution.

Figure 6 shows a result of the proposed method. Figure 6(a) and (b) are the standard model and scan data, respectively. Figure 6(c) is the result of the skeleton-based initial deformation and Figure 6(d) is the final result. As the Figure indicates, the initial deformation process ensured that even a high-resolution standard model with different posture would produce results that approximated the shape of the scan data. One can also see that performing a detailed deformation using the initial posture deformation results created a human-body model with an even closer resemblance to the shape of the scan data. Also, Figure 6(e) shows the result of increasing the resolution of Figure 6(d). As in Figure 6(d), it can be confirmed the result is close to the shape of scan data.

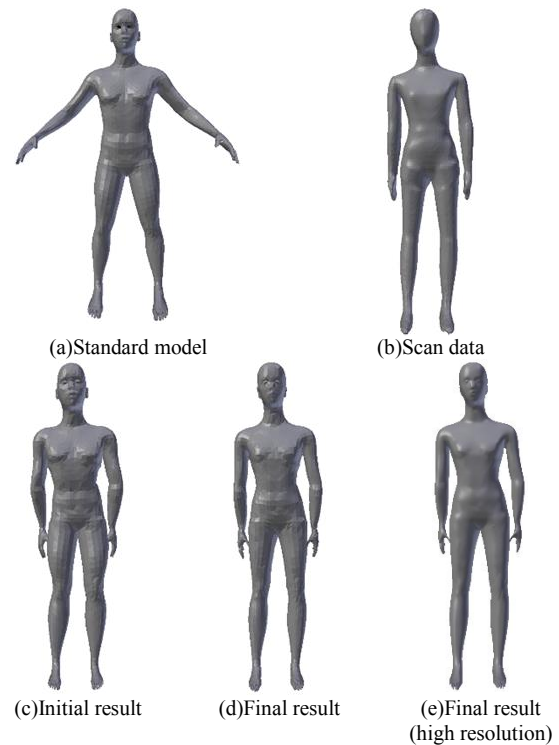


Figure 6: Modeling with the proposed method

### 3.3. Position Specification

Below is an overview of the process for identifying a specified position on the human-body model.

1. Use an RGB-D sensor to detect specified positions pointed by a laser pointer
2. Convert the specified positions detected in step 1 to coordinates on the human-body model
3. Obtain the position on the human-body model

To maximize operability in actual autopsy settings, we allow the medical examiner uses a laser pointer to illuminate and thereby specify the positions of sites where he or she intends to record findings. By then using an RGB-D sensor to detect the specified positions, our method automatically calculates the corresponding positions on the human-body model.

We detect a position that the medical examiner has specified with the laser pointer using background subtraction technique. We obtain frame-by-frame images via the RGB-D sensor, and then the position pointed can be detected as the position with large difference from the previous frame. Next we need to convert the position coordinates in the RGB-D sensor coordinate system to the position coordinates of the human-body model. To do so, we use a rigid ICP algorithm to register the predefined skeleton for the standard model and the skeleton obtained via RGB-D sensor and then obtain a transformation matrix for converting coordinates from the RGB-D sensor coordinate system to the human-body model coordinate system.

Figure 7 shows the results of obtaining positions on the human-body model. We can see that using a laser pointer resulted in accurate specified positions and that

the position information on the human-body model conformed to the original specified positions.

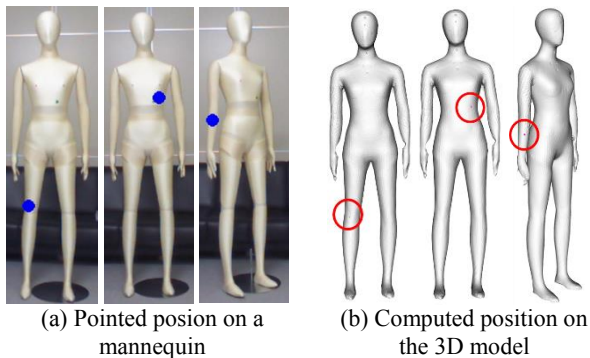


Figure 7: Results of obtaining position information on the human-body model

#### 4. CONCLUDING REMARKS

This study proposes a method for creating a human-body model and obtaining position information on the human-body model for visualizing forensic autopsy data. As shown in Figure 6, although the resulting model presents the shape characteristics of the scan data, the method failed to produce the correct shape of hands. One possible reason is that the smoothness error function  $E_s$  may fall into a local solution for the fingers. We will try to introduce some structure aware method for solving this problem. Currently the algorithm has only been tested in the laboratory by scanning a mannequin with a RGB-D sensor. We plan to evaluate and improve the method by applying it to real autopsy site.

#### 5. ACKNOWLEDGEMENT

This work was supported by JSPS Grants-in-Aid for Scientific Research KAKENHI (JP26240015).

#### 6. REFERENCES

- [1] Patric, L., Calle, W., Anders, P., Claes, L. and Anders Y.: Full Body Virtual Autopsies Using a State-of-the-art Volume Rendering Pipeline, proceedings of TVCG, Vol. 12, No. 5, pp. 869-876(2006).
- [2] Boussejra, M. O., Adachi, N., Shojo, H., Takahashi, R., Fujishiro, I.: LMML: Initial developments of an integrated environment for forensic data visualization, EG/IEEE VGTC Conference on Visualization (EuroVis Short Papers), pp.31-35 (2016).
- [3] Xi, P., Guo, H. and Shu, C.: Human Body Shape Prediction and Analysis Using Predictive Clustering Tree, proceedings of the 2011 International Conference on 3D Imaging, Modeling, Processing, Visualization and Transmission(3DIMPVT '11), pp. 196-203(2011).
- [4] Angelov, D., Srinivasan, P., Koller, D., Thrun, S., Rodgers, J., Davis, J.: SCAPE: Shape Completion and Animation of People. ACM SIGGRAPH, Volume. 24, Issue. 3, Pages. 408-416(2005).
- [5] Allen, B., Curless, B. and Popovic, Z.: The space of human body shapes: reconstruction and parametrization from range scans, proceedings of ACM SIGGRAPH, Vol. 22, Issue. 3, pp. 587-594(2003).
- [6] David, D., Jorg, S. and Sven, B.: Learning to interpret pointing gestures with a time-of-flight camera, proceedings

HRI '11 of the 6th international conference on Human-robot interaction, pp. 481-488(2011).

[7] Krzysztof, P., Anastasia, K., James R, W. and Edward L.: Smartcasting: a discount 3D interaction technique for public displays, proceedings of the 26th Australian Computer-Human Interaction Conference on Designing Futures: the Future of Design, pp. 119-128(2014).

[8] Huang, Q., Koltun, V. and Guibas, L.: Joint shape segmentation with linear programming, proceedings of ACM SIGGRAPH Asia, Vol. 30, Issue. 6, Article. No. 125(2011).

[9] Catmull, E., and Clark, J.: Recursively Generated B-Spline Surfaces on Arbitrary Topological Meshes, Computer Aided Design 10, 6, 350-355(1978).